CHINESE OPTICS LETTERS

Vol. 20, No. 7 | July 2022

Low-threshold continuous operation of fiber gas Raman laser based on large-core anti-resonant hollow-core fiber

Xinyue Zhu (朱昕玥)[1,2], Fei Yu (于 飞)[2,3*], Dakun Wu (吴达坤)[3], Yan Feng (冯 衍)[2,3], Shufen Chen (陈淑芬)[1], Yi Jiang (江 毅)[1], and Lili Hu (胡丽丽)[2,3]

[1] School of Optics and Photonics, Beijing Institute of Technology, Beijing 100081, China

[2] Shanghai Institute of Optics and Fine Mechanics, Chinese Academy of Sciences, Shanghai 201800, China

[3] Hangzhou Institute for Advanced Study, UCAS, Hangzhou 310024, China

*Corresponding author: yufei@siom.ac.cn

Received March 5, 2022 | Accepted April 18, 2022 | Posted Online May 7, 2022

Continuous operation of fiber gas Raman lasing at the 1135 nm wavelength is experimentally demonstrated with an output power exceeding 26 W. Rotational stimulated Raman scattering (Rot-SRS) is generated in the hydrogen gas filled 50 m homemade anti-resonant hollow-core fiber (AR-HCF). A single-frequency fiber laser at the 1064 nm wavelength is used as the pump source, and a minimum threshold of 31.5 W is measured where the core diameter of AR-HCF reaches 37 μm. Up to 40.4% power conversion efficiency of forward Rot-SRS is achieved in the single-pass configuration, corresponding to a quantum efficiency of 43.1%. Over 1 W strong backward Rot-SRS is observed in the experiment, ultimately limiting the further increase of Rot-SRS generation in the forward direction.

Keywords: anti-resonant hollow-core fiber; fiber gas laser; rotational stimulated Raman scattering.
DOI: 10.3788/COL202220.071401

1. Introduction

Gas-filled microstructured hollow-core fibers (MS-HCFs) have demonstrated many advantages as a minimized gas cell and shown the promising potential of reforming the bulky gas laser[1] and sensors into a more compact and robust all-fiber configuration[2]. The gas–light interaction along MS-HCF could be possibly enhanced by 10^6 times stronger than that in the Rayleigh zone of the free-space laser beam[3]. In MS-HCF, both the gas and light field could be tightly confined in a core region of tens of μm^2 area. Meanwhile, its effective interaction length depending on the fiber loss is much extended to tens of meters. The latest development of anti-resonant hollow-core fiber (AR-HCF) demonstrated 0.22 dB/km minimum fiber loss that implies more than a thousand effective length to use[4].

The stimulated Raman scattering (SRS) of gas was first observed, to the best of our knowledge, in 1963[5], which is proven as an effective method to generate new wavelengths especially in the ultraviolet and mid-infrared spectral ranges[6,7]. Both hollow capillaries[8] and high-finesse cavities[9] were often used to reduce the pump threshold, while the Stokes conversion efficiency was still weak around 5%[9].

In 2002[3], SRS in H_2-filled Kagome hollow-core fiber (Kagome-HCF) was successfully demonstrated, and a record of 30% conversion efficiency of the Stokes wave at the 683 nm wavelength was measured using a pulsed laser source (532 nm, pulse duration 6 ns) as the pump. Such a leap of conversion efficiency gave birth to the concept of the fiber gas Raman laser (FGRL)[10–24].

Given the nature of SRS, the *Q*-switched pulsed laser of nanoseconds of pulse duration is often preferred as the pump of the FGRL, where the high peak power and narrow linewidth are favorable for low threshold and high slope efficiency. Pumped by a *Q*-switched microchip laser at 1 μm, FGRL based on vibrational SRS (Vib-SRS) of H_2 at 1.9 μm was demonstrated in 2014[20], with a maximum quantum conversion efficiency of 48%. In 2016[21], Vib-SRS output at 1553 nm was generated in the C_2H_6-filled AR-HCF with a 38% conversion efficiency reported, pumped by a microchip laser at 1064 nm with a linewidth of 6 pm and a maximum peak power of about 400 kW. Recently, Edelstein and colleagues explored the use of SF_6 and CF_4 in the FGRL by pumping with a high peak power *Q*-switched fiber laser at the 1030 nm wavelength[22].

In spite of continuous interest in the pulsed FGRL, continuous-operation FGRL was seldom reported. Lack of proper pump sources with spectral brightness comparable with the pulsed laser makes the CW SRS threshold a challenge to reach. In 2007[17], Benabid *et al.* firstly reported, to the best of our knowledge, the continuous running of rotational-SRS (Rot-SRS) of H_2 gas filled in a photonic-bandgap hollow-core fiber (PBG-HCF)

by pumping with a single-frequency fiber laser at 1064 nm. The brightness of the pump source reached 250 W/MHz with a linewidth less than 100 kHz. Later, they successfully raised the continuous output up to 55 W[18]. It is noted that in both works, the PBG-HCFs with a small core of 6 μm in diameter played an important role, where the spatially tight confinement of light contributed to the effective reduction of the lasing threshold.

In this Letter, we report the continuous Rot-SRS lasing in H_2-filled AR-HCF in a single-pass configuration with a large-core diameter exceeding 35 μm for the first time, to the best of our knowledge. Up to 26 W of Rot-SRS output at 1135 nm was demonstrated, pumped by a circularly polarized single-frequency fiber laser at 1064 nm with 10 kHz linewidth. A maximum slope efficiency of 40.3% was obtained in a 50 m fiber length filled with 2.5 bar (1 bar = 10^5 Pa) H_2 gas. The threshold of FRGL was measured as 31.5 W. We found that the emergence of backward Rot-SRS and the cascaded Rot-SRS would ultimately limit the FRGL output.

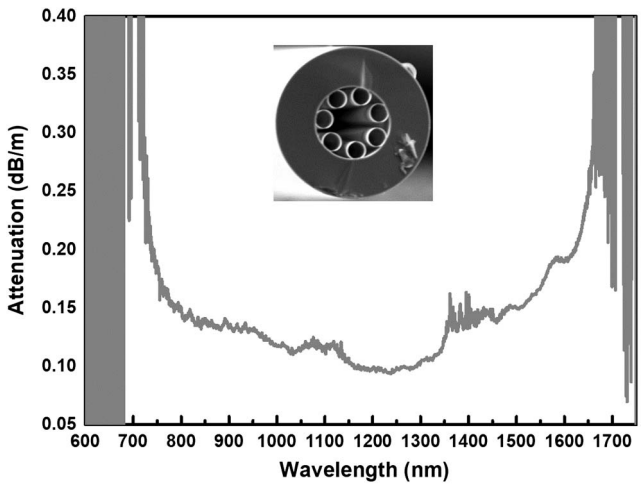

Fig. 1. Measured attenuation of AR-HCF by a cut-back from 96.8 m to 22 m. Inset: SEM picture of AR-HCF. The core diameter is about 35 μm.

2. Experimental Setup

The homemade AR-HCF in this paper was fabricated by the stack-and-draw technique method, using Heraeus F300 fused silica tubes, as shown in the inset of Fig. 1. The cladding of AR-HCF consists of seven capillaries, with an average capillary diameter of about 17 μm and core wall thickness of around 335 nm. The fiber attenuation was measured by a cut back and around 0.11 dB/m and 0.13 dB/m at 1064 nm (pump wavelength) and 1135 nm (first Stokes of Rot-SRS) wavelengths, respectively. The core diameter of AR-HCF is about 35 μm, and the fundamental-like mode diameter at 1064 nm wavelength is simulated around 26 μm.

Figure 2 shows the schematic of the experiment setup. The pump source was a homemade single-frequency continuous fiber laser operating at the 1064 nm wavelength, with a linewidth of 10 kHz and a maximum output power above 70 W[25]. The laser output is linearly polarized and near diffraction limited with an M^2 of 1.2. A $\lambda/4$ waveplate (QWP) is used before the incidence of AR-HCF to convert the linearly polarized laser beam into circular polarization to enhance the Rot-SRS effect. A 4-f lens system is applied to scale the pump beam size, and, finally, around 80% coupling efficiency at pump wavelength at the incident end of AR-HCF was realized.

The single-pass FGRL consists of a 50 m AR-HCF, as shown in Fig. 2. The AR-HCF was loosely rewound on a steel plate in a circle with a radius of about 50 cm to avoid any notable bend loss[26]. The two fiber ends were mounted in homemade gas cells and air-tight sealed. The whole length of AR-HCF could be vacuumed and pressurized via the gas cells. Cooling water was circulated inside the shell of the gas cell for heat management.

Before the incident end of the AR-HCF, a sampler (M1) (9:1) was used to monitor the pump power and collect the possible backward laser beam with a long-pass filter (LPF) together. Coated sapphire glass plates were used as the windows of gas cells with transmission efficiencies of 99% and 98.5% at 1064 nm and 1135 nm, respectively.

At the output end, the laser beam was collimated by the lens (L4) and then characterized by the thermal power meter, optical fiber spectrometer (Ideaoptics NIR2500), and pyroelectric array

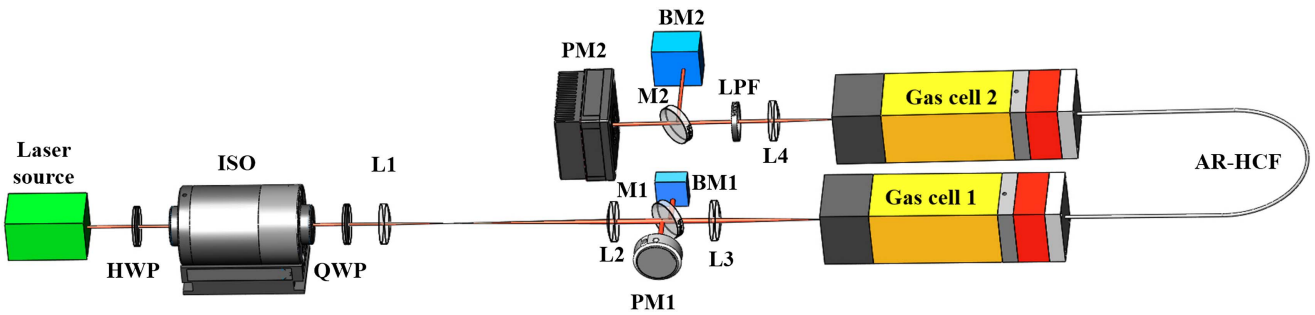

Fig. 2. Schematic of the laser delivery setup. HWP is half wave plate; ISO is isolator; QWP is quarter wave plate; L1, L2, L3, L4 are coated aspherical lenses with f_1 = 50 mm, f_2 = 150 mm, f_3 = 90 mm, f_4 = 50 mm; M1 is a sampler to monitor the power of the laser source and backward Stokes light; M2 is another sampler used to monitor the output power and beam profile or wavelength at the same time; PM1, PM2 are power meters. At BM1 and BM2 positions, pump and Stokes laser beams were characterized by using a power meter, optical spectral analyzer, and pyroelectric array camera, respectively.

camera (Pyrocam IIIHR), respectively. Another LPF was used to separate the Stokes laser from the residual pump, with an average 97% transmission efficiency at wavelengths longer than 1100 nm and $< 10^{-4}$ at 1064 nm (FELH1100).

3. Result and Discussion

In our experiment, the dependence of SRS on hydrogen pressure is explored at 2.5, 5, 7.5, and 10 bar, respectively. Typical spectra of forward emission at 5 bar for different pump powers are shown in Fig. 3. Figure 4 are the corresponding far-field beam patterns at the pump and Rot-SRS wavelengths. We attribute the slightly degraded output beam profile to the stress applied on AR-HCF when mounted by V-grooves in the gas cell.

As shown in Fig. 3, the cascaded Rot-SRS (RS2) at 1216 nm could be measured by the spectrometer at high pump power over 60 W while it was too weak for the thermal meter to respond. Vib-SRS at 1907 nm failed to be found for any H_2 pressure, even when the pump power rose to 70 W. We attribute the absence of Vib-SRS to (1) the circular polarization of the pump that is expected to effectively suppress the Vib-SRS[27] and

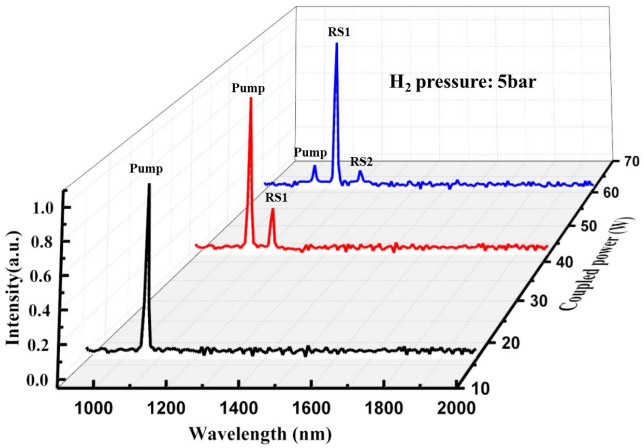

Fig. 3. Measured output spectra in the forward direction under 5 bar gas pressure for different pump power. Pumped at 1064 nm, the first rotational Stokes laser (RS1) of H_2 is at 1135 nm, and the second rotational Stokes (RS2) at 1216 nm.

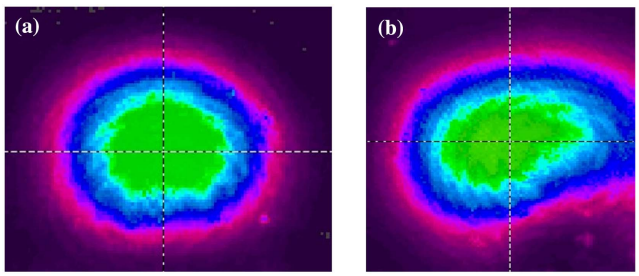

Fig. 4. Far-field patterns at (a) 1064 nm and (b) 1135 nm measured at the output end of AR-HCF at 5 bar gas pressure.

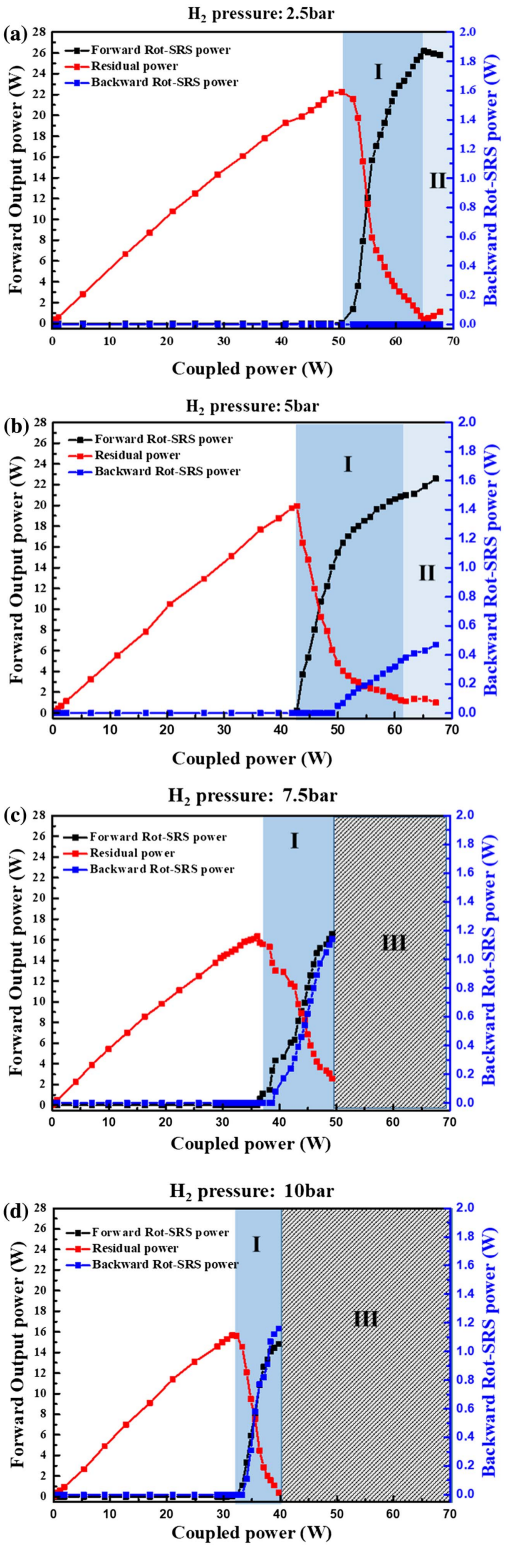

Fig. 5. Measured powers of the residual pump and forward and backward Rot-SRS as a function of coupled pump power with a H_2 pressure at (a) 2.5 bar, (b) 5 bar, (c) 7.5 bar, and (d) 10 bar. In Region (I), Rot-SRS in the forward and backward directions is measured only; (II) bi-directional first Rot-SRS and forward second Rot-SRS, (III) the pump laser failed to work because strong backward Rot-SRS is disturbed. The forward Rot-SRS power (black line) and residual power (red line) refer to the left axis, and the backward Rot-SRS power (blue line) refers to the right axis.

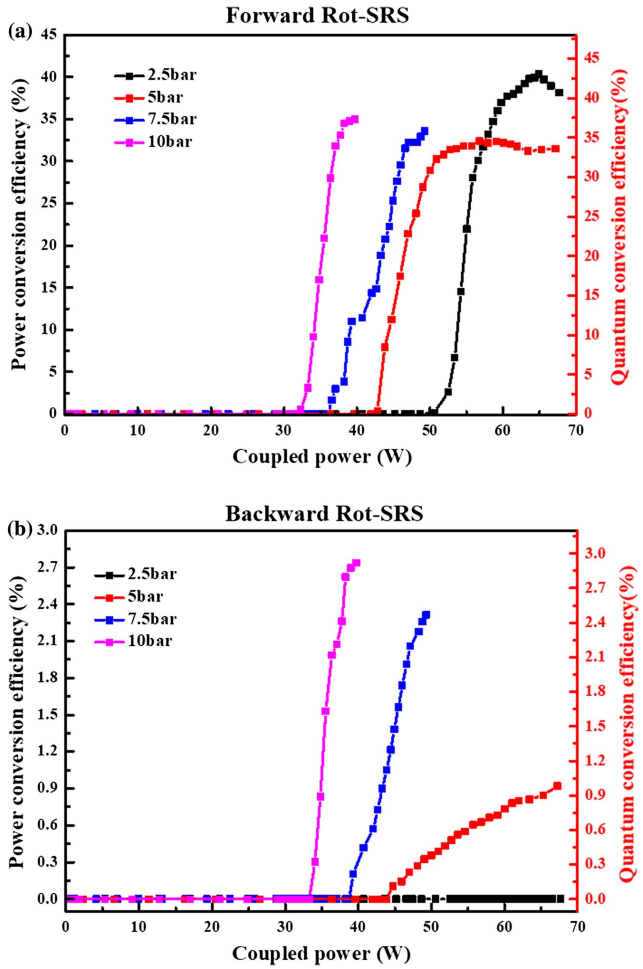

Fig. 6. Power (left axis) and quantum conversion efficiency (right axis) of (a) forward Rot-SRS and (b) backward Rot-SRS as a function of coupled pump power at different gas pressures.

(2) 1 dB/m high loss at 1907 nm that is almost ten times of that at 1135 nm.

Figure 5 summarizes the power of the Stokes and residual pumps as a function of coupled pump power measured by a power meter. In the experiment, an LPF was used to record the Stokes power, and the residual pump power was then calculated by subtracting the total power of the Stokes from the total output.

In Region I of Fig. 5, only the forward and backward Rot-SRS Stokes were measured at all pressures. At higher pump power, the cascaded second Rot-SRS started to appear in Region II but remained weak in the forward direction at 2.5 and 5 bar pressures. In Region III, the pump laser failed before the cascaded Rot-SRS because the quick rise of Rot-SRS in the backward direction strongly interfered with the pump laser operation. In Fig. 6, conversion efficiencies of bidirectional Rot-SRS are replotted from the data in Fig. 5.

The maximum output of forward Rot-SRS appeared at 2.5 bar pressure, with a conversion efficiency of 40.4%. At higher pressures, despite a reduced threshold from 50.6 W down to 31.5 W, the rising of backward Rot-SRS started to compete and exhausted the gain of the single pass. Moreover, the backward Rot-SRS resulting in the pump failure also stopped the potentially higher FRGL output.

According to the threshold formula[18],

$$P_{\mathrm{th}} = \frac{A_{\mathrm{eff}} G_{\mathrm{th}}}{g_s L_{\mathrm{eff}}} = \frac{A_{\mathrm{eff}} G_{\mathrm{th}}}{g_s} \frac{\alpha_p}{1 - \exp(-\alpha_p L)}, \tag{1}$$

where A_{eff} is the effective area of the modal field, g_s is the peak steady-state Raman gain coefficient, and α_p is the fiber attenuation at the pump wavelength. At bending, extra loss of AR-HCF gives rise to a shorter effective length, resulting in a higher threshold. Based on the characterized pump thresholds for

Table 1. Comparison of Pump Thresholds in H_2-Filled FGRLs under Continuous and Pulsed Operation.

	Pump Source Type	Fiber Core Diameter (μm)	Loss (dB/m)	Gas Pressure (bar)	Threshold Power (W)	Normalized Pump Threshold ($W \cdot MHz^{-1} \cdot \mu m^{-2}$)
This paper	CW	30	0.11 dB/m at 1064 nm; 0.13 dB/m at 1135 nm	10	31.5	5.93
F. Couny *et al.* in 2007[17]	CW	5	0.1 dB/m at 1064 nm; 0.14 dB/m at 1135 nm	5	2.25	1.125
F. Couny *et al.* in 2010[18]	CW	6	0.1 dB/m at 1061 nm; 0.14 dB/m at 1131 nm	15	37	13.09
W. Huang *et al.* in 2020[13]	Pulse (10 ns)	9	0.016 dB/m at 1550 nm; 0.03 dB/m at 1700 nm	16	40 (peak power)	24.8
H. Li *et al.* in 2020[29]	Pulse (12 ns)	9	0.04 dB/m at 1540 nm; 0.11 dB/m at 1700 nm	16	50 (peak power)	25.18

different pressures, when we assume that the pump power threshold rises to 70 W, the losses should increase to 0.15 dB/m, 0.18 dB/m, 0.21 dB/m, and 0.25 dB/m for 2.5 bar, 5 bar, 7.5 bar, and 10 bar pressures, respectively. According to our simulation of AR-HCF, the corresponding minimal bend radii are estimated as 7.6 cm, 6.3 cm, 5.8 cm, and 5.4 cm, respectively.

The maximum power of backward Rot-SRS reached 1.16 W at 10 bar pressure, with quantum efficiency close to 3%. Our continuous backward SRS generated in the experiment is much more efficient than reported previously[17,18]. In Fig. 6, the measured thresholds of backward Rot-SRS were very close to the forward, implying a strong backward gain comparable with the forward. The tendencies of bi-directional Rot-SRS conversion are found very similar with the noise-seeded bi-directional Vib-SRS in Ref. [28] pumped by a *Q*-switched laser at 532 nm.

In Table 1, we summarize and compare the pump thresholds of H_2-filled FRGLs in the continuous and typical pulsed operations[13,18,19,29]. By normalizing the threshold with the core area and pump laser linewidth, we find that the continuous pumping could be more efficient in terms of pump power utilization. It is noted that the pressure broadening effect and effective fiber length are not included in the normalization process.

4. Conclusion

In conclusion, we demonstrated a low threshold and efficient Rot-SRS in H_2-filled large-core AR-HCF in a single-pass configuration at 1135 nm. A maximum power conversion efficiency of 40.3% was achieved by using a 50 m length of fiber filled with 2.5 bar H_2, and the maximum power reached 26.2 W. The noise-seeded backward Rot-SRS was observed with a maximum power of 1 W. A lower pressure is favorable to suppress the backward Rot-SRS, which competes with the forward counterpart and limits further increase of FRGL output.

Acknowledgement

This work was partly supported by the International Science and Technology Cooperation Program (No. 2018YFE0115600), National Natural Science Foundation of China (No. 61935002), Chinese Academy of Sciences (No. ZDBS-LY-JSC020), and National Key R&D Program of China (Nos. 2020YFB1312802 and 2020YFB1805900). F. Yu was supported by the CAS Pioneer Hundred Talents Program.

References

1. H. Bao, W. Jin, and H. L. Ho, "Tuning of group delay with stimulated Raman scattering-induced dispersion in gas-filled optical fiber," Chin. Opt. Lett. **18**, 060601 (2020).
2. Z. Zhang, Y. Wang, M. Zhou, J. He, C. Liao, and Y. Wang, "Recent advance in hollow-core fiber high-temperature and high-pressure sensing technology [Invited]," Chin. Opt. Lett. **19**, 070601 (2021).
3. F. Benabid, J. C. Knight, G. Antonopoulos, and P. St.J. Russell, "Stimulated Raman scattering in hydrogen-filled hollow-core photonic crystal fiber," Science **298**, 399 (2002).
4. H. Sakr, T. D. Bradley, G. T. Jasion, E. N. Fokoua, S. R. Sandoghchi, I. A. Davidson, A. Taranta, G. Guerra, W. Shere, Y. Chen, J. R. Hayes, D. J. Richardson, and F. Poletti, "Hollow core NANFs with five nested tubes and record low loss at 850, 1060, 1300 and 1625 nm," in *Optical Fiber Communications Conference and Exhibition* (2021), p. 1.
5. R. W. Minck, R. W. Terhune, and W. G. Rado, "Laser stimulated Raman effect and resonant four-photon interactions in gases H_2, D_2, and CH_4," Appl. Phys. Lett. **3**, 181 (1963).
6. D. J. Brink and D. Proch, "Efficient tunable ultraviolet source based on stimulated Raman scattering," Opt. Lett. **7**, 494 (1982).
7. A. D. Papayannis, G. N. Tsikrikas, and A. A. Serafetinides, "Generation of UV and VIS laser light by stimulated Raman scattering in H_2, D_2, and H_2/He using a pulsed Nd:YAG laser at 355 nm," Appl. Phys. B **67**, 563 (1998).
8. P. Rabinowitz, A. Kaldor, R. Brickman, and W. Schmidt, "Waveguide H_2 Raman laser," Appl. Opt. **15**, 2005 (1976).
9. L. S. Meng, K. S. Repasky, P. A. Roos, and J. L. Carlsten, "Widely tunable continuous-wave Raman laser in diatomic hydrogen pumped by an external-cavity diode laser," Opt. Lett. **25**, 472 (2000).
10. F. Benabid, G. Bouwmans, J. C. Knight, P. St.J. Russell, and F. Couny, "Ultrahigh efficiency laser wavelength conversion in a gas-filled hollow core photonic crystal fiber by pure stimulated rotational Raman scattering in molecular hydrogen," Phys. Rev. Lett. **93**, 123903 (2004).
11. Z. Wang, F. Yu, W. J. Wadsworth, and J. C. Knight, "Efficient 1.9 μm emission in H_2-filled hollow core fiber by pure stimulated vibrational Raman scattering," Laser Phys. Lett. **11**, 105807 (2014).
12. M. S. Astapovich, A. V. Gladyshev, M. M. Khudyakov, A. F. Kosolapov, M. E. Likhachev, and I. A. Bufetov, "Watt-level nanosecond 4.42 μm Raman laser based on silica fiber," IEEE Photonics Technol. Lett. **31**, 78 (2019).
13. W. Huang, Z. Li, Y. Cui, Z. Zhou, and Z. Wang, "Efficient, watt-level, tunable 1.7 μm fiber Raman laser in H_2-filled hollow-core fibers," Opt. Lett. **45**, 475 (2020).
14. Y. Cui, W. Huang, Z. Li, Z. Zhou, and Z. Wang, "High-efficiency laser wavelength conversion in deuterium-filled hollow-core photonic crystal fiber by rotational stimulated Raman scattering," Opt. Express **27**, 30396 (2019).
15. F. Benabid, G. Antonopoulos, J. C. Knight, and P. St.J. Russell, "Stokes amplification regimes in quasi-cw pumped hydrogen-filled hollow-core photonic crystal fiber," Phys. Rev. Lett. **95**, 213903 (2005).
16. F. Benabid, F. Couny, J. C. Knight, T. A. Birks, and P. St.J. Russell, "Compact, stable and efficient all-fiber gas cells using hollow-core photonic crystal fibers," Nature **434**, 488 (2005).
17. F. Couny, F. Benabid, and P. S. Light, "Subwatt threshold CW Raman fiber-gas laser based on H_2-filled hollow-core photonic crystal fiber," Phys. Rev. Lett. **99**, 143903 (2007).
18. F. Couny, B. J. Mangan, A. V. Sokolov, and F. Benabid, "High power 55 watts CW Raman fiber-gas-laser," in *CLEO and QELS 2010 Conference* (2010), paper CTuM3.
19. Y. Cui, Z. Zhou, W. Huang, Z. Li, and Z. Wang, "Quasi-all-fiber structure CW mid-infrared laser emission from gas-filled hollow-core silica fibers," Opt. Laser Technol. **121**, 105794 (2020).
20. Z. Wang, F. Yu, W. J. Wadsworth, and J. C. Knight, "Efficient 1.9 μm emission in H_2-filled hollow core fiber by pure stimulated vibrational Raman scattering," Laser Phy. Lett. **11**, 105807 (2014).
21. Y. Chen, Z. Wang, B. Gu, F. Yu, and Q. Lu, "Achieving a 1.5 μm fiber gas Raman laser source with about 400 kW of peak power and a 6.3 GHz linewidth," Opt. Lett. **41**, 5118 (2016).
22. S. Edelstein and A. A. Ishaaya, "High-efficiency Raman conversion in SF_6- and CF_4-filled hollow-core photonic bandgap fibers," Opt. Lett. **44**, 5856 (2019).
23. S. Gao, Y. Wang, W. Ding, and P. Wang, "Hollow-core negative-curvature fiber for UV guidance," Opt. Lett. **43**, 1347 (2018).
24. F. Yu, M. Xu, and J. C. Knight, "Experimental study of low-loss single-mode performance in anti-resonant hollow-core fibers," Opt. Express **24**, 12969 (2016).
25. X. Zeng, S. Cui, J. Qian, X. Cheng, J. Dong, and J. Zhou, "10 W low-noise green laser generation by the single-pass frequency doubling of a single-frequency fiber amplifier," Laser Phys. **30**, 075001 (2020).

26. R. M. Carter, F. Yu, W. J. Wadsworth, J. D. Shephard, T. Birks, J. C. Knight, and D. P. Hand, "Measurement of resonant bend loss in anti-resonant hollow core optical fiber," Opt. Express **25**, 20612 (2017).
27. M. R. Perrone, G. D. Nunzio, and C. Panzera, "Competition between vibrational and rotational Raman scattering in H_2," Opt. Commun. **145**, 128 (1998).
28. M. K. Mridha, D. Novoa, and P. St.J. Russell, "Dominance of backward stimulated Raman scattering in gas-filled hollow-core photonic crystal fibers," Optica **5**, 570 (2018).
29. H. Li, W. Huang, Y. Cui, Z. Zhou, and Z. Wang, "Pure rotational stimulated Raman scattering in H_2-filled hollow-core photonic crystal fibers," Opt. Express **28**, 23881 (2020).